Italian Journal of Engineering Geology and Environment
www.ijege.uniroma1.it

A NEAR REAL-TIME FORECASTING SYSTEM FOR SHALLOW LANDSLIDES AT REGIONAL SCALE BASED ON DISTRIBUTED MODELLING AND WEATHER PREDICTIONS

Elena Benedetta MASI(*), Guglielmo ROSSI(**), Nicolò BRILLI(*) & Veronica TOFANI(*)

(*)University of Florence - Department of Earth Sciences - Florence, Italy
(**)University of Florence - Civil Protection Centre - Florence, Italy
Corresponding author: elenabenedetta.masi@unifi.it

EXTENDED ABSTRACT

Le frane superficiali indotte da precipitazioni intense costituiscono una fra le più gravose fonti di pericolo e danni alle comunità montane, a causa della loro frequente e diffusa occorrenza, della rapidità dei processi di mobilizzazione che le contraddistingue e dell'assenza, nella maggior parte dei casi, di segnali premonitori riconoscibili antecedenti l'innesco.

Tali fenomeni sono generalmente controllati da variazioni rapide della pressione neutra della copertura detritica, indotte da eventi pluviometrici di breve durata ed elevata intensità. La previsione dell'innesco di tali frane su scala regionale risulta particolarmente complessa in contesti caratterizzati da marcata eterogeneità geomorfologica, litologica, geotecnica e climatica. In tali contesti emergono i limiti degli approcci empirici basati su soglie pluviometriche in quanto a trasferibilità spaziale, la disponibilità di inventari di frana ampi e dettagliati non risulta sufficiente a colmare l'intrinseca incapacità di tali metodologie di rappresentare in modo esplicito i processi fisici che governano la risposta idro-meccanica dei versanti.

In questo lavoro è presentato lo sviluppo di un prototipo di sistema di previsione delle frane superficiali pluvio-indotte, basato su modellazione fisicamente basata e distribuita, progettato per operare in tempo reale a scala regionale. Il sistema di previsione è basato sull'utilizzo del modello di stabilità dei versanti HIRESSS (*HIgh REsolution Slope Stability Simulator*) e di previsioni meteorologiche di precipitazione ed è in grado di generare mappe di probabilità di innesco delle frane superficiali ad alta risoluzione spaziale e temporale in ristretti tempi di calcolo. Il sistema è stato calibrato per l'Area di Allerta B della Regione Autonoma Valle d'Aosta (circa 800 km² di estensione), caratterizzata da elevata suscettibilità a fenomeni di instabilità superficiale innescati da eventi pluviometrici intensi.

Le attività di ricerca hanno riguardato: (*i*) l'ottimizzazione del modello HIRESSS in termini di efficienza computazionale ed affidabilità dei risultati, finalizzata al suo impiego in un contesto operativo continuo; (*ii*) la calibrazione del sistema sulla base delle caratteristiche idrologiche, geotecniche, morfologiche e climatiche dell'area di studio, mediante *back analysis* di eventi di frana documentati; (*iii*) lo sviluppo di procedure automatiche per l'acquisizione e l'integrazione continua delle previsioni meteorologiche e per la produzione di output sia distribuiti che spazialmente aggregati.

HIRESSS è un simulatore distribuito fisicamente basato che accoppia un modulo idrologico basato su una soluzione analitica semplificata dell'equazione di Richards, con un modulo geotecnico basato su approccio del pendio indefinito. HIRESSS considera le variazioni della suzione matriciale e l'effetto del rinforzo radicale sulla resistenza al taglio dei terreni. L'incertezza associata ai parametri idrologici e geotecnici è gestita mediante simulazioni Monte Carlo.

Il sistema di previsione è operativo da giugno 2024 e utilizza come input dinamico le previsioni di precipitazione fornite dal modello meteorologico ICON-CH1. Su base giornaliera vengono prodotte mappe distribuite di probabilità di innesco delle frane superficiali per il giorno corrente e per quello successivo, insieme a prodotti aggregati a scala di sottobacino, resi disponibili attraverso una piattaforma webGIS. Gli output distribuiti, calcolati con risoluzione spaziale di 10 m e risoluzione temporale di 3 ore, sono aggregati sulla base di unità territoriali di tipo sottobacino mediante un approccio a doppia soglia, basato sulla probabilità di innesco e sul numero minimo di pixel instabili. La calibrazione delle soglie di aggregazione è stata effettuata attraverso validazione per mezzo di inventari di frane osservate in occasione di eventi pluviometrici significativi.

Il prototipo del sistema di previsione rappresenta un avanzamento sostanziale verso l'implementazione di un sistema di allertamento regionale in tempo reale per frane superficiali basato su modellazione fisicamente basata e previsioni meteorologiche.

IJEGE, Special Issue 1, (2026): 163-174, DOI: 10.4408/IJEGE.2026-01.S-16
E-ISSN 2035-5688 | ISSN 1825-6635 / ©Author(s)

ABSTRACT

This work presents the development of a forecasting system for shallow rainfall-induced landslides, designed to provide daily near–real-time outputs at a regional scale. The system integrates hydrological and slope stability distributed modelling with daily rainfall forecasts from a weather prediction model to generate daily shallow landslide initiation forecasts for an area of hundreds of square kilometers.

Research activities focused on: *i*) the optimization of the HIRESSS model to enhance computational efficiency and physical consistency for real-time forecasting; (*ii*) the calibration of the system based on the hydrological, geotechnical, morphological and climatic characteristics of the study area; and (*iii*) developing algorithms enabling the continuous use of meteorological forecasts and the production of both distributed (grid-based) and aggregated (sub-basin) outputs.

The operational system based on the HIRESSS model has been active since June 2024 for the Alert Zone B of the Aosta Valley Region. It uses precipitation forecasts from the ICON-CH1 weather prediction model as dynamic input. The system generates landslide initiation susceptibility maps in terms of failure probability, with a 10 m spatial and 3-hour temporal resolution, producing forecastsfor the current and following day. Additionally, it provides aggregated probabilities at sub-basin level through a calibrated threshold system, supporting early warning activities.

Recent developments have focused on optimizing the real-time dissemination of model outputs through an open-data platform ensuring transparency, accessibility, and operational usability for regional authorities and decision-makers. The developed system represents a significant step toward a fully operational landslide early warning system at the regional scale based on physically based distributed modelling and meteorological forecasting.

Keywords: *landslide prediction, shallow landslides, distributed modelling, real-time landslide forecasting, regional modelling*

INTRODUCTION

Shallow rainfall-induced landslides are among the most widespread and recurrent natural hazards in hilly and mountainous regions, posing persistent threats to infrastructure, human activities, and public safety. Their triggering mechanisms are strongly controlled by short-term rainfall dynamics, resulting in rapid and spatially widespread initiation with limited premonitory signs. In alpine environments, characterized by steep slopes, shallow soils, and strong spatial variability in hydrological, geotechnical, and land-cover properties, these phenomena pose a major challenge for regional risk management and civil protection activities.

Landslide forecasting and early warning systems have been widely developed over the last decades, adopting approaches based on *i*) empirical methods to define rainfall thresholds or *ii*) physically based modelling. Empirical methods are widely adopted in operational contexts of regional extension (Aleotti, 2004; Martelloni *et alii*, 2012; Lagomarsino *et alii*, 2013), as they provide relatively efficient tools for landslide prediction and warning, with limited data and computational requirements. However, their applicability and reliability are constrained by limited transferability to areas lacking robust calibration datasets, as well as by their inability to explicitly represent the physical processes governing slope instability (Bordoni *et alii*, 2019). These limitations are particularly critical at the regional scale, where strong heterogeneity in morphology, lithology, and geotechnical properties is present.

Conversely, physically based distributed models simulate slope stability processes through mathematical relationships linking the geotechnical, hydrological, and morphometric characteristics of the analyzed slope portion. Although their demonstrated reliability, their operational use for near–real-time forecasting is still limited (Pack *et alii*, 2001; Baum *et alii*, 2002, 2010; Lu & Godt, 2008; Simoni *et alii*, 2008; Arnone *et alii*, 2011; Salciarini *et alii*, 2017; Park *et alii*, 2013; Rossi *et alii*, 2013). High computational demand, uncertainties in parameterization at large scales, and the difficulty of continuously integrating meteorological forecasts have hindered their adoption within regional early warning systems.

Nowadays, increasing reliability and availability of weather prediction data have significantly widened the potential for forecast-based landslide warning. However, fully operational systems combining physically based distributed modelling and rainfall forecasts at regional scale remain scarce. The effective integration of meteorological forecasts into a landslide forecasting system that has to provide reliable results in near-real time, requires a powerful slope stability simulator whose structure is optimized for the purpose, in addition to a robust regional-scale calibration, and procedures to translate distributed model outputs into information usable by decision-makers.

This study presents the development of a regional-scale forecasting system for shallow rainfall-induced landslides based on a physically based model (HIRESSS, Rossi *et alii*, 2013) designed to operate in near real-time using weather predictions. Specific objectives include: (*i*) optimizing the HIRESSS model for real-time applications; (*ii*) calibrating the system considering hydrological, geotechnical and climatic characteristics of the study area (a portion of the Aosta Valley Region, Nothern Italy); and (*iii*) developing procedures for continuous forecast updating and for the generation of both distributed and aggregated outputs.

The presentation of the forecasting system represents an entirely novel contribution, such as some aspects of both optimisation and calibration of HIRESSS model, while other aspects of the latter represent a consolidated foundation from prior studies (Masi *et alii*, 2023; Tofani *et alii*, 2023, Salvatici *et alii*, 2018). For completeness and reader accessibility, these are revisited here to motivate choices carried out during development and set-upping of the forecasting system or to compare results of the present study. Where previously presented, they are enriched by new quantitative data, comparative validations, and analytical visualizations not included in previous publications.

STUDY AREA

The Valle d'Aosta region is administratively subdivided into four natural hazard alert zones for civil protection and risk management purposes. The study area corresponds to the eastern alert zone, named "Alert Zone B," and covers an area of 837 km² (Fig. 1).

The Valle d'Aosta region covers an area of approximately 3,200 km² within the Western Alpine chain. The region belongs to the Europe-vergent Austroalpine–Penninic structural domain and includes a complex of tectono-metamorphic units arranged in a nappe system. The geological setting reflects post-collisional Alpine tectonics and ongoing neotectonic activity.

The territory is geomorphologically characterized by steep slopes and deeply incised valleys shaped by Quaternary glacial and fluvial processes. U-shaped valleys, glacial deposits, and alluvial fans are features widespread throughout the area. The main drainage system is represented by the Dora Baltea River and its tributaries.

The region is highly susceptible to slope instabilities due to pronounced relief energy and significant precipitation. Landslide processes include rockfalls, deep-seated gravitational slope deformations, debris flows, debris avalanches, and shallow slides, frequently triggered by intense rainfall events. Land cover is typical of Alpine regions, with forests, natural grasslands, and rocky outcrops with sparse or absent vegetation on the slopes and human settlements concentrated along valley bottoms.

Mean annual precipitation ranges from about 500–700 mm/year along the main valley floor to 900–1,100 mm/year in the surrounding mountainous areas. Rainfall maxima typically occur in spring and autumn, and winter precipitation is largely dominated by snowfall at elevations above 1,500–2,000 m a.s.l. (Centro Funzionale, Regione Autonoma Valle d'Aosta, 2025; StatsClimat, 2025).

In the last decades, occurrence of short-duration, high-intensity rainfall events has increased, and events with cumulative precipitation commonly exceeding 150–250 mm over 48–72 hours and peak hourly intensities locally above 20–30 mm/h have recorded (ANSA Valle d'Aosta, 2025 - January 17; ANSA Valle d'Aosta, 2025 - May 2).

The study area Alert Zone B encompasses three principal valleys: the Champorcher Valley, the Gressoney (or Lys) Valley, and the Ayas Valley. The Champorcher Valley (west-east oriented) is situated in the southern sector of the study area on the right-orographic side of the Dora Baltea. The Gressoney and Ayas valleys (predominantly north–south oriented) are situated in the

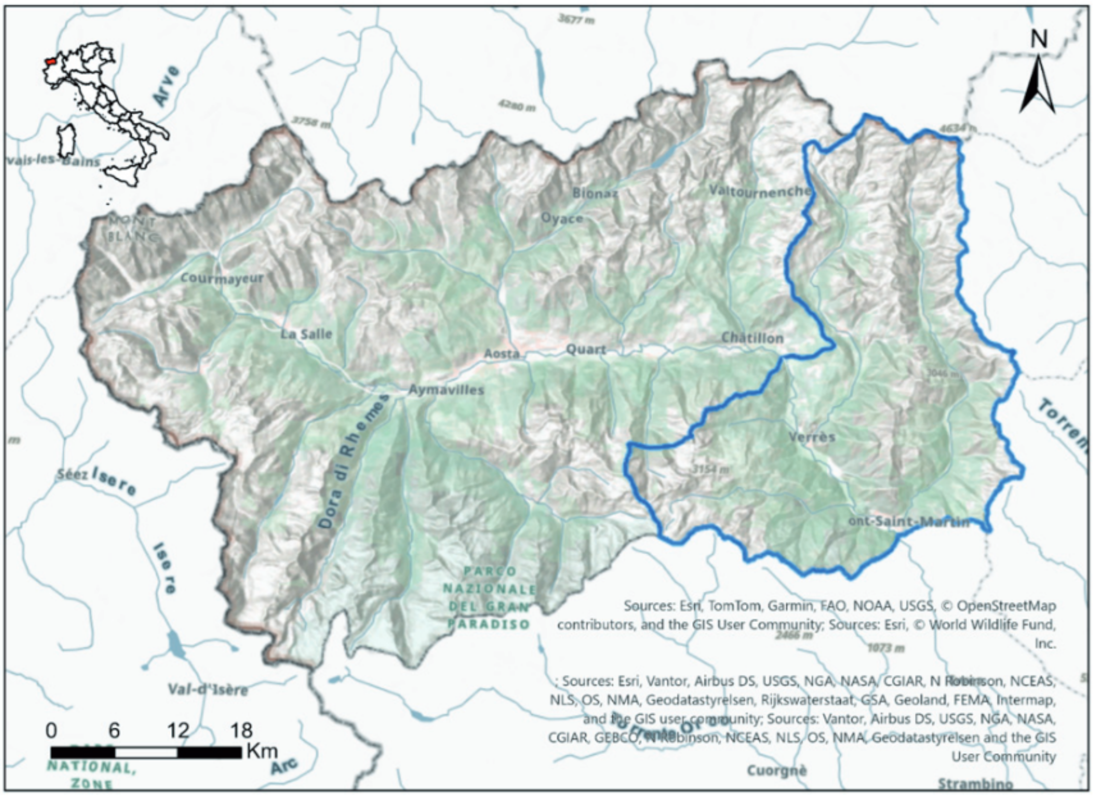

Fig. 1 - Study area (highlighted in blue): Alert zone B of Valle d'Aosta region

north sector and are bounded to the north by the Monte Rosa Massif (4,527 m a.s.l.) and to the south by the Dora Baltea River (Fig. 1).

The geomorphological and lithological characteristics, and the frequent intense rainfall to which it is subjected make Alert Zone B an ideal test area for the prototype real-time landslide forecasting system, providing a representative setting to evaluate model performance and potential operational use.

MATERIALS AND METHODS

The HIRESSS simulator (Rossi *et alii*, 2013) was selected as the distributed model for slope stability analyses within the forecasting system. The model requires both static and dynamic input data to perform stability simulations. Static inputs consist of spatially distributed geotechnical and morphometric parameters, while dynamic inputs are represented by rainfall intensities associated with the investigated event. Static parameters considered are slope gradient, effective cohesion (c'), root cohesion (c_r), friction angle (φ'), dry unit weight (γ_d), soil thickness (d_{bt}), hydraulic conductivity (k_s), initial soil saturation (S), pore size index (λ), bubbling pressure (h_b), effective porosity (n), residual water content (q_r), eventual outcrop rock mask and rainfall intensity. Rainfall intensities fed to the model can be represented by recorded data (by radar and/or rain gauges) in case of back analyses, or whether predictions.

Details about data collection and values adopted for the geotechnical parameters about Alert Zone B are presented in Salvatici *et alii*, 2018 and Masi *et alii*, 2023.

In the following sections details about the model, and activities carried out for its optimization and calibration are presented.

Hiresss Model

The HIRESSS model was selected for the slope stability analyses of the forecasting system due to its suitability for near–real-time applications. Actually, the model was originally developed to address real-time landslide forecasting requirements. For this purpose, the code was designed to be strongly parallelized, allowing efficient exploitation of multi-processor architectures and a significant reduction in computational time, which is essential for operational applications at regional scale. In addition to this, the suitability for the purposes is due to its main features including: (*i*) time-dependent computation of the factor of safety during rainfall events; (*ii*) variable-depth slope stability analysis; (*iii*) consideration of soil suction under unsaturated conditions; (*iv*)

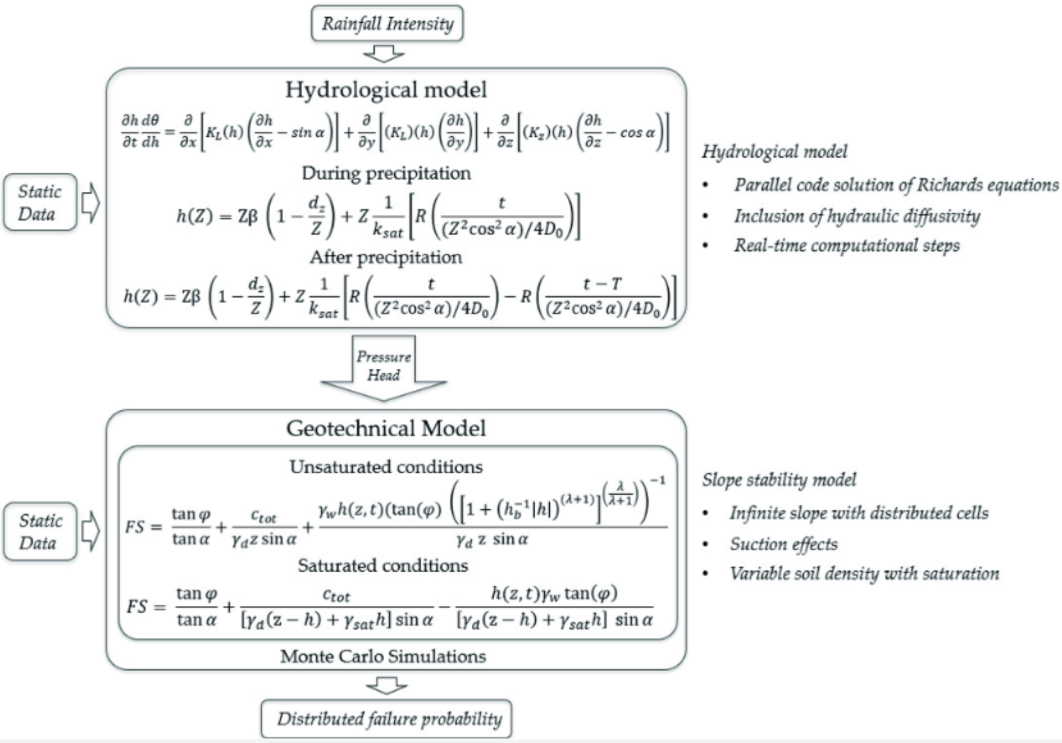

Fig. 2 - Hiresss model structure and main characteristics. Hydrological model: h is the groundwater pressure head, θ is the soil water volumetric content, t is time, α is the slope angle, K_L and K_Z are respectively the hydraulic conductivity in the lateral directions (x and y) and the hydraulic conductivity in slope-normal direction (z), D_0 is the maximum diffusivity, β is a factor depending on rainfall intensity rate (considering Darcy's law for vertical flow in response to infiltration) and K_Z, d_Z is the steady water table, T is the rainfall duration and R is the response function. Geotechnical model: F_S is factor of safety, φ is the friction angle, α the slope angle, γd the dry soil unit weight, γw the water unit weight, h the pressure head, hb is the bubbling pressure and λ the pore size index distribution and γsat is the saturated soil unit weight

probabilistic treatment of uncertainties in hydrological and geotechnical parameters through Monte Carlo simulations.

Specifically, HIRESSS is a physically based distributed model composed of a hydrological and a geotechnical module (Fig. 2). The hydrological module processes rainfall as dynamic input and computes pressure head variations, which are transferred to the geotechnical module to evaluate slope stability in terms of failure probability. The model structure is inspired by IVERSON (2000) and is conceptually similar to TRIGRS. The hydrological component is based on an analytical solution of a simplified Richards equation under wet conditions (BAUM *et alii*, 2002; SIMONI *et alii*, 2008), expressed through a hydraulic diffusivity formulation. The geotechnical module adopts an infinite slope approach that accounts for unsaturated soil behavior, including the effects of matric suction on shear strength. HIRESSS had been recently modified to consider the effect of the root reinforcement to the stability of slopes (MASI *et alii*, 2023; MASI *et alii*, 2021). The model has been successfully applied in various geological and geomorphological settings (ROSSI *et alii*, 2013; TOFANI *et alii*, 2017; SALVATICI *et alii*, 2018; CUOMO *et alii*, 2020; MASI *et alii*, 2023).

Recently, the efficiency of HIRESSS in simulating shallow landslide initiation in the Valle d'Aosta region was demonstrated in a study in which its performance was compared with that of the distributed slope stability model Scoops3D (BRILLI *et alii*, 2024).

Model optimization

The activities carried out to optimize the HIRESSS model for a real-time application mainly focused on two aspects: defining the appropriate number of Monte Carlo iterations for the real-time forecasting system requirements; assessing the effect of rainfall interception by canopies in the context of application of the model. The latter was investigated to evaluate the potential integration of this process and thereby improve the forecasting performance of the system.

The HIRESSS models allows for flexibility in several configuration aspects, including the number of Monte Carlo iterations adopted to account for uncertainty in hydrological and geotechnical input parameters. In view of the operational requirements of the forecasting system, 1000 iterations were set for the simulations based on the results of a study previously performed (MASI *et alii*, 2023) to define the best compromise of number of iterations between computational speed and output reliability. In that study, a sensitivity test had been made for the same study area of the forecasting system, by simulating the rainfall event recorded between 2 and 30 April 2009. Four simulations had been carried out by varying the number of Monte Carlo iterations (10, 100, 1000, and 10000), while all static input parameters had been unchanged. The results of this test are summarised Table 1 (simulation results compared in terms of daily number of unstable pixels, defined as grid cells exhibiting a maximum landslide initiation probability exceeding 80% within 24 hours, and overall processing times).

Since model outputs stabilized after 1000 iterations, the processing time required for simulations with this number of iterations was assessed considering the time steps of the rainfall forecasts that the system had to use every morning and found to be compatible with real-time application requirements.

A study focused on the evaluation of rainfall interception by vegetation in the study area was carried out. This assessment was designed to determine whether such an effect could significantly influence precipitation in the study area, thus justifying an update of the model to include this process among the modeled hydrogeological phenomena. Multiple tests were performed by applying interception models available in the literature to a rainfall event (26–28 April 2009), during which 24h cumulative precipitation reached a maximum of approximately 208 mm in Alert zone B (rainfall data from rain gauges): interception was estimated using the methodologies proposed by CUOMO *et alii* (2021) and WU *et alii* (2019) (Fig.3).

In CUOMO *et alii* (2021), the effective vegetation interception is computed on a daily basis according to the formulation of Aston (1979), which assumes that interception depends on the maximum canopy storage capacity (Smax), the canopy openness parameter, and the cumulative rainfall since the beginning of the event. To simplify the requirement for specific input data needed to solve Aston's equation, the study area was assumed to be entirely covered by broadleaf forests, with a Leaf Area Index (LAI) set equal to 3 and canopy openness equal to 0.9. The estimated interception corresponds

Iterations (shoots)	Δ Unstable pixels (mean)	Processing time (h)
10	–	5.4
100	− 100,000	7.7
1,000	− 25,000	39.1
10,000	≈ 0	350.7

Tab. 1 - Sensitivity of unstable pixel estimates to the number of Monte Carlo iterations for the 2009 rainfall event (02 April 2009–30 April 2009), Valle d'Aosta study area. Δ Unstable pixels (mean) represents the average change in the number of unstable pixels relative to the previous iteration level (negative values indicate a reduction), differences refer to the average number of unstable pixels computed for the same days of the event (a pixel was considered unstable when its factor of safety (FS) was < 1.2, for each time step, the model performs multiple FS calculations, and a failure probability (FP) is assigned as the percentage of iterations in which FS < 1.2, a pixel was classified as unstable with FP >80% based on previous HIRESSS applications (ROSSI et alii, 2013; SALVATICI et alii., 2018). Data from MASI et alii,2023) to the maximum canopy storage capacity for a broadleaf forest, i.e., approximately 0.9 mm. This result is consistent with the theoretical assumption of the applied equation, according to which, for cumulative rainfall tending to infinity, the estimated interception approaches the maximum storage capacity.

To account for the spatial variability of vegetation cover within the study area, the methodology proposed by Wu *et alii* (2019) was also applied. This approach simulates interception using the Aston (1979) equation, while Smax is estimated according to the formulation by De Roo *et alii* (1996). In his study, Smax was estimated as a function of the LAI: for the different land cover types present in Alert Area B, LAI values were derived from Knote *et alii* (2009). In this case, the estimated interception values were higher than those obtained with the method of Cuomo *et alii* (2021), reaching a maximum of approximately 3 mm (Fig. 3).

In this case study, both methodologies indicate that modeled vegetation interception is negligible relative to daily cumulative rainfall. Thus, incorporating it into the HIRESSS model would not yield predictive improvements justifying implementation. 2009 and October 2020) triggering multiple landslides had been considered: the failure probability maps aggregated using different combinations of thresholds were validated considering shallow landslides occurred during the events.

Simulation results relating to one of the two events (April 2009) had been previously validated (Masi *et alii,* 2020; Tofani *et alii,* 2023). During that event, specifically between 26 and 28 April 2009, a maximum of cumulative precipitation of 268 mm had been recorded in Region Valle d'Aosta (Lillianes Granges station), including 208 mm on 27 April. Within alert Area B, nine landslides relevant to shallow slope instability had been identified.

In the present study, a further extreme rainfall event was considered (October 2020): the event hit the Region between 2 and 3 October 2020, with daily precipitation exceeding 200 mm at several stations and peak hourly intensities up to 45 mm/h. Among the 53 hydrogeological phenomena recorded, 12 landslides were considered suitable for aggregation calibration.

Coherently with Masi *et alii* 2020 and Tofani *et alii* 2023, Hiresss simulation of October 2020 was performed using

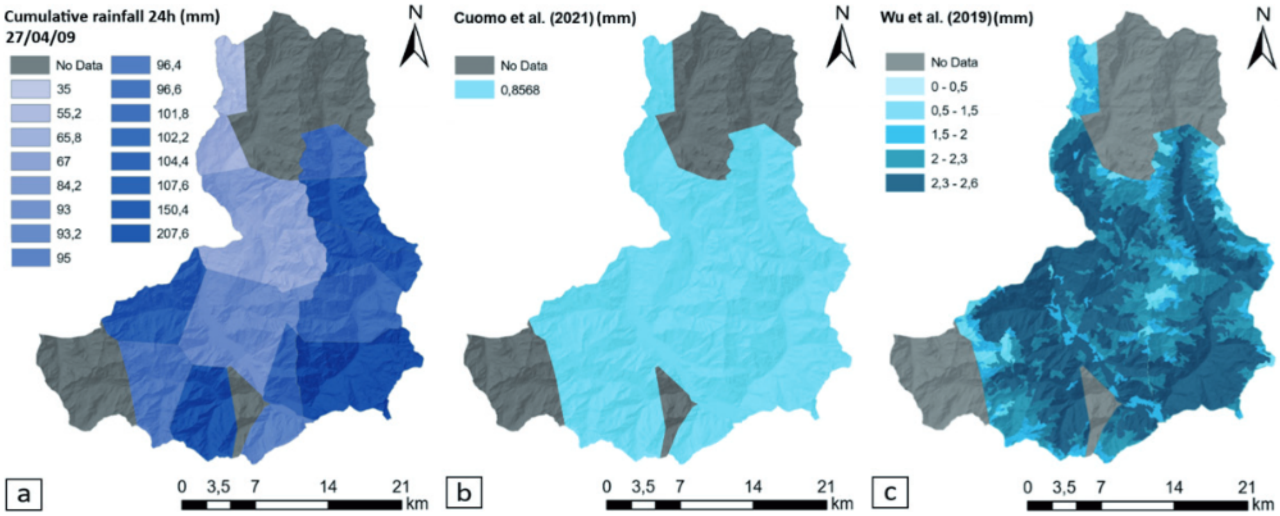

Fig. 3 - Comparison of (a) 24h cumulative rainfall on 27/04/2009; (b) 24h rainfall interception by canopies computed with Cuomo *et alii (2021); (c) 24h rainfall interception by canopies computed with* Wu *et alii (2019)*

Thresholds definition for spatial aggregation

In view of the objective of an operational use of the forecasting system, a spatial aggregation of the distributed failure probability data is needed. In this study the spatial aggregation was carried out using territorial units represented by subbasins such as previously carried out in Masi *et alii,* 2020, and Tofani *et alii*, 2023. Subbasins were classified as stable or unstable based on whether the number of pixels exceeded a failure probability threshold.

Number of pixels and failure probability thresholds were defined through a back-analysis approach. Results of HIRESSS simulations relating two different intense rainfall events (April 1,000 Monte Carlo iterations and a spatial resolution of 10 m, and results aggregation was carried out using territorial units (subbasins) with an average area of approximately 0.37. The subbasins had been defined based on a 10 m resolution Digital Terrain Model, and size of the units had been defined to be compatible with the average dimensions of landslides recorded in the regional inventory (2002–2020), while minimizing loss of spatial detail (Tofani *et alii*, 2023). Since the simulation of a further event was carried out to improve/confirm the thresholds calibration previously performed, coherence with the previous studies was guaranteed.

For the back analysis of HIRESSS outputs, the 24-hour maximum failure probability map of 3 October was used for aggregation of the October 2020 event (for the event April 2009 was the 24-hour maximum failure probability map of April 27), as the temporal accuracy of the landslide occurrence data did not allow for the use of hourly outputs.

Model performance was evaluated through spatial comparison between unstable subbasins and observed landslides, contingency tables and ROC curve were constructed (Table 2 and Fig. 4).

Regarding event 2009, aggregation had been tested using a fixed triggering-probability threshold of 80% combined with pixel-number thresholds of 250, 300, and 350 pixels, and the 80%/250 pixel combination had been achieved the highest true positive rate (88.9%), correctly identifying 8 out of 9 landslides, at the expense of a higher false positive rate (13.9%)(Tofani *et alii,* 2023).

Regarding event 2020, the three aggregation configurations tested were: 80%/230 pixels, 80%/250 pixels, and 50%/450 pixels.

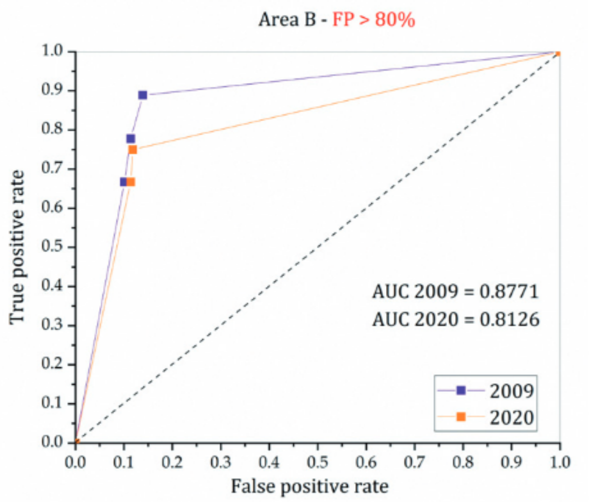

Fig. 4 - ROC curve and AUC of the validated simulations for the 2009 and 2020 events in Alert Area B

The 80%/230 pixels combination provided the best compromise, yielding a true positive rate of 75% and a false positive rate of 12%. Compared to the 2009 event, performance was slightly reduced, likely due to the exceptional intensity of the 2020 rainfall and differences in landslide localization accuracy, suggesting that extreme events may require event-specific aggregation strategies.

THE REAL-TIME LANDSLIDE FORECASTING SYSTEM PROTOTYPE

Final activities of the study focused on the development and operationalization of the forecasting system. This phase specifically involved the automation of rainfall data acquisition, the continuous execution of HIRESSS simulations, and the aggregation of model outputs, namely, the pixel-based landslide triggering probability calculated for each simulated rainfall time step, into defined territorial units (subbasins). These units were subsequently classified according to the double-threshold procedure (pixel number / probability threshold) calibrated for each alert area under study.

During the development process, several routines were evaluated both for the continuous retrieval of rainfall data to be supplied to the model and for the post-processing phase, including the aggregation of outputs. The goal of this testing was to identify the approaches that ensured maximum efficiency and consistency, minimizing the risk of delays or errors in the workflow. Once the desired performance was achieved in terms of both computational speed and reliability, the forecasting system was formally deployed.

The real-time forecasting system has been fully operational since 25 June 2024, functioning continuously (Fig. 5). Each morning, the system automatically retrieves rainfall forecasts in GeoTIFF format from a dedicated FTP server. These forecasts are produced by the ICON-CH1 meteorological model. Each GeoTIFF file contains 16 bands, representing cumulative rainfall predicted over consecutive three-hour intervals, starting from 00:00–03:00 (band 1) up to a 48-hour accumulation (band 16).

Event	FP/ Number of unstable pixels	TP	FN	TN	FPS
2009	**80/250**	88.9% (8/9)	11.1% (1/9)	86.1% (1120/1300)	13.9% (180/1300)
	80/300	77.8% (7/9)	22.8% (2/9)	88.6% (1152/1300)	11.4% (148/1300)
	80/350	66.7% (6/9)	33.3% (3/9)	89.9% (1169/1300)	10.1% (131/1300)
2020	**80/230**	75% (9/12)	25% (3/12)	87.6% (1319/1505)	11.8% (186/1505)
	80/250	66.7% (8/12)	33.3% (4/12)	88.6% (1333/1505)	11.4% (172/1505)
	50/450	75% (9/12)	25% (3/12)	85.8% (1292/1505)	14.2% (213/1505)

Tab. 2 - Contingency matrix for the validation of the model results. "FP/pixels number" represents the combination between the thresholds of FP and number of pixels to consider a basin as unstable (i.e. at least × pixels with a FP higher than y); "TP" is the true positive percentage (correct alarms) i.e. the unstable areas correctly localized by the simulation (the number of unstable basins found by the model with at least one landslide inside it with respect to the actual total unstable basins); "FN" is the false negative percentage (missing alarms) i.e. the unstable areas not localized by the model (the number of the stable basins found by the model with at least one actual landslide inside it with respect to the total actual unstable basins); "TN" is the true negative percentage (correct non-alarms) i.e. the areas correctly defined stable by the model (the basins found stable by the model without landslides inside it compared to the actual total stable basins); "FPS" is the false positive percentage (incorrect alarms) i.e. the areas incorrectly defined stable by the model (unstable basins found by the model without landslides inside it compared to the total actual stable basins). Data of 2009 event from Tofani et alii 2023

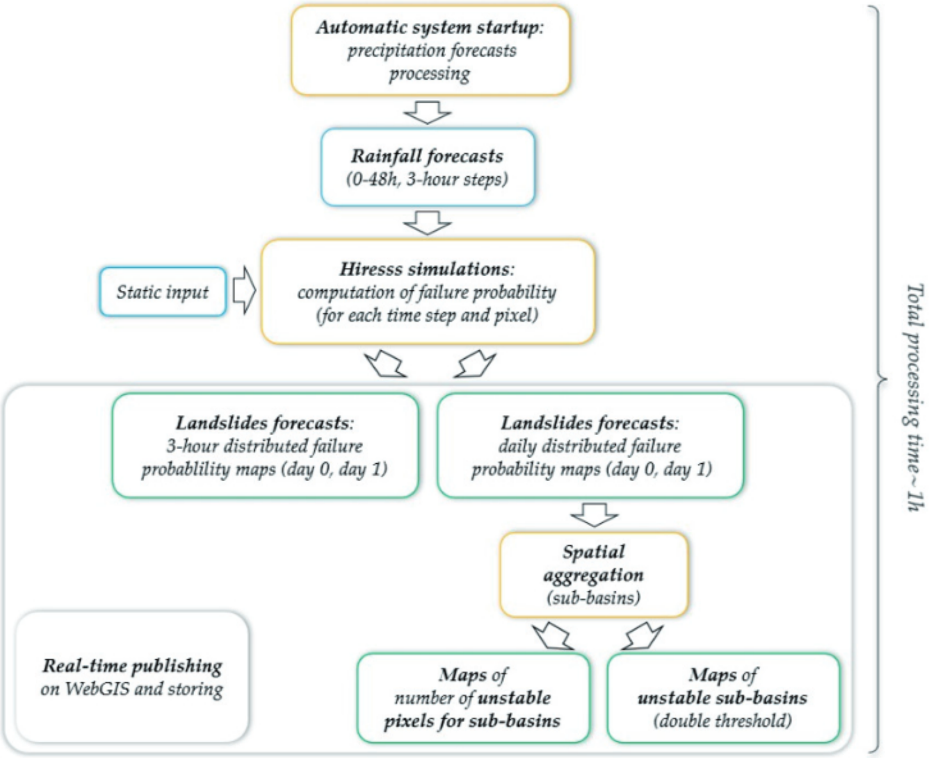

Fig. 5 - Near real time forecasting system workflow. In orange processing steps, in blue input data, in green model outputs

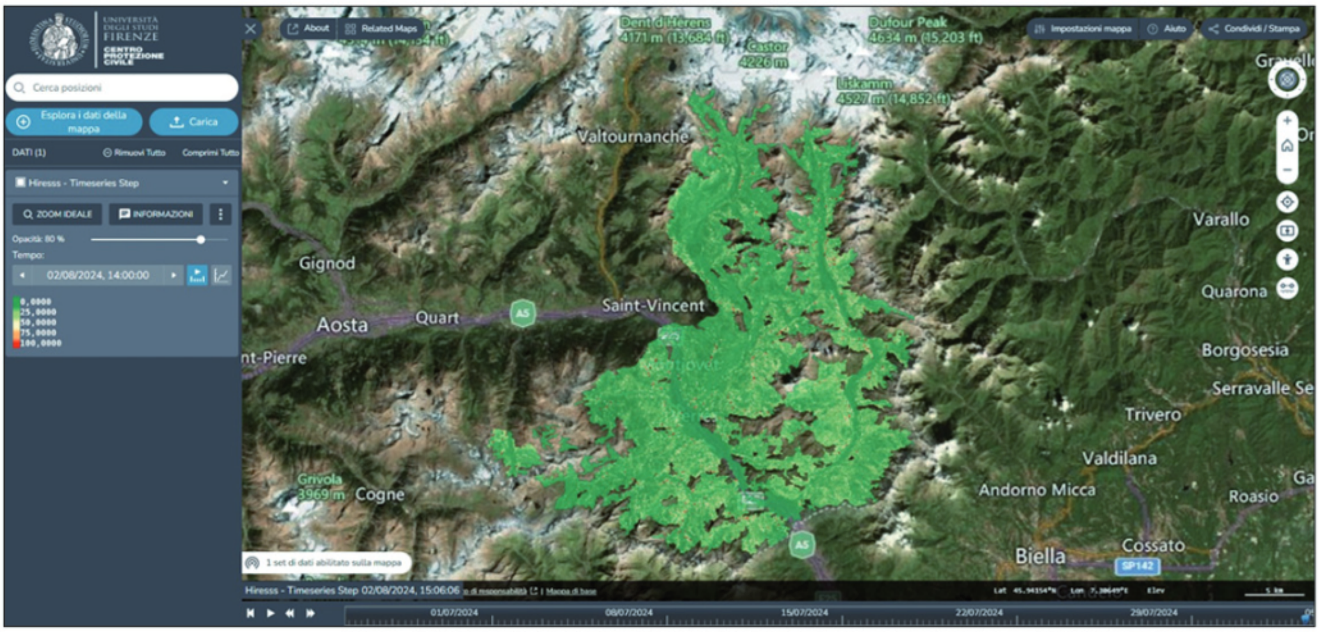

Fig. 6 - A WebGIS platform screen displaying a distributed failure probability map calculated by HIRESSS for Alert Area B

Upon retrieval, the system converts the 16-band GeoTIFFs into individual raster maps of cumulative rainfall for each three-hour interval. These raster maps are then resampled to align precisely with the spatial resolution of the static input data (10×10 m).

Once the rainfall maps are prepared as dynamic input, the system executes HIRESSS simulations with 1,000 Monte Carlo iterations. At the end of the simulation, the system produces 16 three-hourly failure probability maps, along with two daily maps

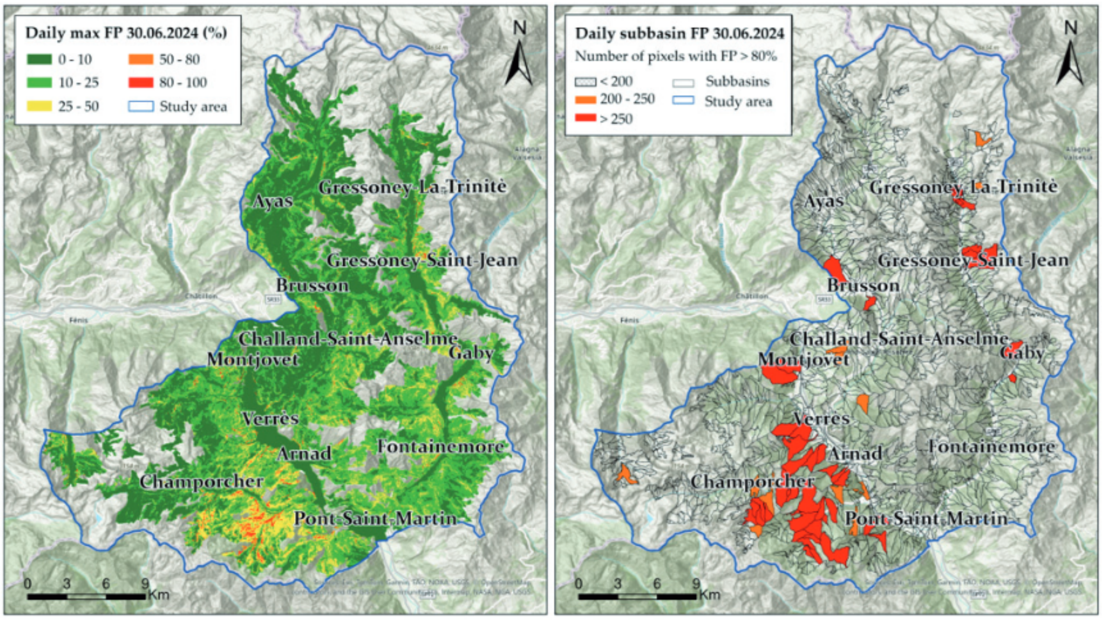

Fig. 7 - Forecasting system outputs. Left: pixel-based daily failure probability (FP) map for June 30, 2024 (for each pixel the highest failure probability computed by HIRESSS during the day based on ICON-CH1 weather forecast is reported). Right: daily FP for each subbasin for June 30, 2024, based on the pixel-based map (for each subbasin the number of pixels with a daily max FP higher than 80% is reported)

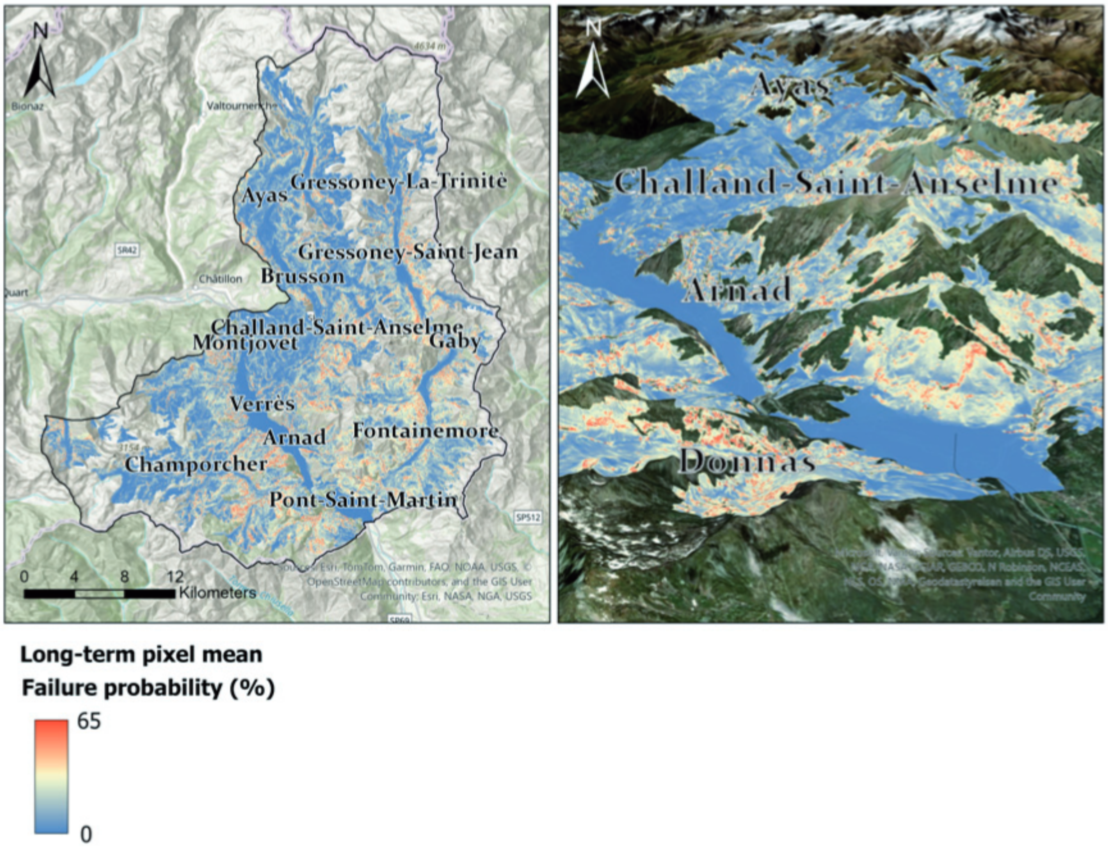

Fig. 8 - Distribution of the long-term mean failure probability (FP), computed for each pixel as the mean of the daily maximum failure probabilities (the maximum FP of each pixel computed by the model during the day) estimated by the model over the period June 2024–October 2025. Left: overview of the study area in two dimensions, right: close-up view of the study area in three dimensions

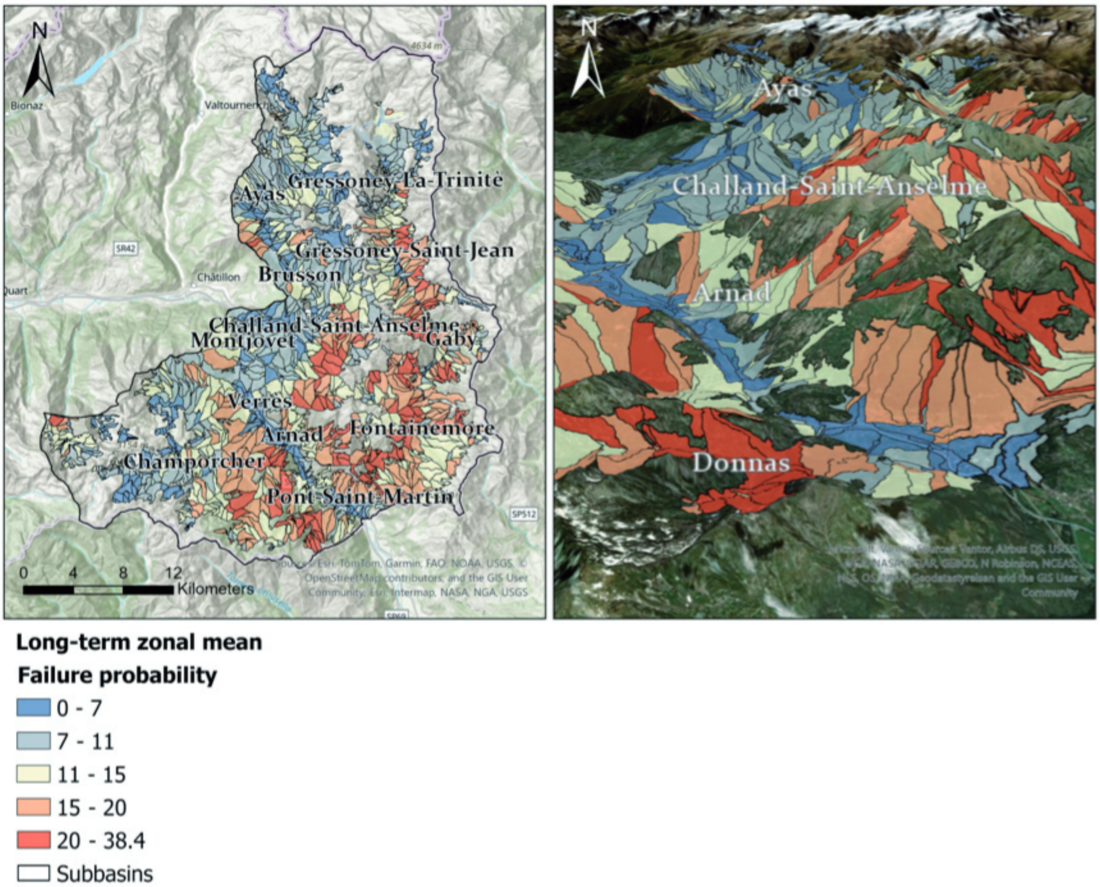

Fig. 9 - Subbasins long-term mean failure probability of the period June 2024–October 2025, computed as the zonal average of pixel-level long-term means. Left: overview of the study area in two dimensions, right: close-up view of the study area in three dimensions

showing the maximum probability predicted for each pixel for the two forecasted days. These outputs are automatically uploaded to a webGISplatform, where they can be explored interactively in 3D or as time series (Fig. 6). In addition, all raster outputs are stored on a server for further analysis and operational use.

In addition to these primary outputs, the system generates two aggregated daily maps based on the calibrated thresholds of failure probability, pixel counts, and territorial units for Alert Zone B (80% probability and 200–250 pixels, (Fig. 7).

The complete workflow (Fig. 5), from data acquisition to map generation, HIRESSS simulation, and uploading to the WebGIS platform and the server, takes approximately one hour to complete using a powerful but several-year-old multiprocessor computer now, with a current machine of affordable cost the time required could drop to ~10 minutes.

Currently, the operational prototype relies exclusively on rainfall forecasts as the dynamic input. Future developments of the system will aim to incorporate real-time rainfall measurements as primary input, with forecasted rainfall serving as supplementary information, further improving the accuracy and timeliness of landslide prediction.

Comprehensive validation of the forecasting system outputs over the operational period (June 2024–October 2025) considering recorded landslide events was not possible at this stage, as the landslide event database of the period is still under completion by the territorial authorities.

To provide a descriptive overview of the long-term behaviour of the forecasting system over the period June 2024–October 2025, the simulated failure probabilities were synthesised as follow: first, daily maximum failure probabilities were temporally averaged at the pixel scale (for each pixel, the long-term mean was computed as the average of the daily maximum failure probabilities estimated over the period June 2024–October 2025); subsequently, these pixel-based long-term means were spatially aggregated at the subbasin scale using zonal averaging (the indicator was obtained by applying a zonal average to the pixel-based long-term mean values) (Fig. 8 e Fig. 9).

CONCLUSIONS

This study presents the development and operational implementation of a regional-scale forecasting system for shallow rainfall-induced landslides based on physically based distributed modelling (HIRESSS) and meteorological precipitation forecasts from the ICON-CH1 model. The prototype has been successfully deployed for Alert Zone B of the Valle d'Aosta region (NW Italy), a high-risk Alpine area of 837 km², and has been fully operational since June 2024, delivering near-real-time assessments of landslide initiation probability at 10 m spatial resolution and 3-hour temporal intervals.

Vegetation interception assessments (using Cuomo *et alii*, 2021 and Wu *et alii*, 2019) confirmed negligible effects (0.9–3 mm of interception vs. ~ 200 mm of 24h cumulative rainfall), avoiding unnecessary model updates to integrate this effect. Event-based back-analyses of 2020 (200 mm 24h cumulative rainfall, 12 shallow landslides) event confirmed calibration of subbasin aggregation thresholds. The 80% failure probability/250-pixel criterion achieved a true positives value of 75% (in case of event 2009 was 88.9%) with a false positives value of 13.9% (in case of event 2009 was 11.8%). ROC analyses confirmed robust performance across events.

The automated workflow ensures operational reliability through a fully streamlined sequence of processes. Each morning, the system automatically retrieves 16-band GeoTIFF rainfall forecasts from the ICON-CH1 meteorological model where each band represents cumulative precipitation over sequential 3-hour intervals (from 00:00–03:00 up to 48-hour totals). These forecasts are processed (converted into three-hours rainfall maps, resampled to align with the 10×10 m resolution of static inputs) and formatted as dynamic rainfall inputs for HIRESSS.

The core simulation phase executes HIRESSS generating in near real time landslide forecasts for the current and the successive days: 16 three-hourly failure probability maps plus two daily maps capturing maximum pixel-level probabilities for the forecast period. Post-processing applies the calibrated dual-threshold aggregation (80% probability/250 pixels for Alert Zone B), classifying subbasins (~0.37 km² average) as stable/unstable and producing actionable indicators for civil protection. All outputs, distributed pixel maps, subbasin summaries, and time-series visualizations, are automatically uploaded to an interactive WebGIS platform (supporting 3D exploration) and archived on a server, completing the end-to-end cycle in approximately 1 hour to enable near-real-time decision-making.

Over the operational period (June 2024–October 2025), long-term synthesis of daily maximum failure probabilities reveals spatially persistent instability hotspots: pixel-scale temporal averaging identifies chronically susceptible terrain while subbasin-scale zonal statistics highlight priority areas for monitoring. This temporal consistency demonstrates system robustness across variable weather conditions, even without comprehensive event validation (pending updated landslide inventories from regional authorities). Such long-term patterns provide valuable baseline hazard zoning, complementing event-specific forecasts and underscoring the prototype's potential for sustained civil protection use.

The shallow landslide forecasting system advances operational landslide early warning by integrating physics-based modelling with forecasts up to 48 hours ahead. Future enhancements will incorporate real-time ground-recorded rainfall data in addition to forecasts, event-specific thresholds for extremes, expansion to other alert zones, and comprehensive performance evaluation as inventories complete.

REFERENCES

ANSA Valle D'aosta (2025, January 17) - *Clima: il 2024, l'anno più piovoso in Valle d'Aosta dal 2000.* Available at: https://www.ansa.it/valledaosta/notizie/2025/01/17/clima-il-2024-lanno-piu-piovoso-in-valle-daosta-dal-2000_7484c117-a53c-4ba1-b80b-65d26325bb50.html

ANSA Valle D'aosta (2025, May 2) - *In media ogni mille anni la pioggia di aprile in Valle d'Aosta.* Available at: https://www.ansa.it/valledaosta/notizie/2025/05/02/in-media-ogni-mille-anni-la-pioggia-di-aprile-in-valle-daosta_b8abd4c6-77d2-416f-b73f-834249dee4b9.html

Arnone E., Noto L., Lepore C. & Bras R. (2011) - *Physically-based and distributed approach to analyze rainfall-triggered landslides at watershed scale.* Geomorphology, **133**: 121-131. https://doi.org/10.1016/j.geomorph.2011.03.019

Baum R.L., Godt J.W. & Savage W.Z. (2010) - *Estimating the timing and location of shallow rainfall-induced landslides using a model for transient unsaturated infiltration.* J. Geophys. Res., **118**:1999. https://doi.org/10.1029/2009JF001321

Baum R.L., Savage W. & Godt J. (2002) - *Trigrs: A fortran program for transient rainfall infiltration and gridbased regional slopestability analysis.* Open-file Report, US Geological Survey.

Bordoni M., Corradini B., Lucchelli L. & Meisina C. (2019) - *Preliminary results on the comparison between empirical and phisically-based rainfall thresholds for shallow landslides occurence.* Italian Journal of Engineering Geology and Environment. Special Issue, **1**: 5-10. https://doi.org/10.4408/IJEGE.2019-01.S-01

Brilli N., Masi E. B., Rossi G. & Tofani V. (2025) - *Slope stability modelling of shallow landslides at a regional scale.* Geoenvironmental Disasters, **12**(1): 18. https://doi.org/10.1186/s40677-025-00323-x

Centro Funzionale, Regione Autonoma Valle D'aosta (2025) - *Climate and influencing factors in the Aosta Valley.* Available at: https://cf.regione.vda.it/en/climate-influencing-factors-in-aosta-valley

Cuomo S., Masi E. B., Tofani V., Moscariello M., Rossi G. & Matano F. (2021) - *Multiseasonal probabilistic slope stability analysis of a large area of unsaturated pyroclastic soils.* Landslides, **18**(4): 1259-1274. https://doi.org/10.1007/s10346-020-01561-w

De Roo A. P. J., Wesseling C. G. & Ritsema C. J. (1996) - *LISEM: a single-event physically based hydrological and soil erosion model for drainage basins*. I: theory, input and output. Hydrological processes, **10**(8): 1107-1117. https://doi.org/10.1002/(SICI)1099-1085(199608)10:8<1107::AID-HYP415>3.0.CO;2-4

Iverson R.(2000) - *Landslide triggering by rain infiltration*. Water Resour. Res., **36**(7): 1897-1910. https://doi.org/10.1029/2000WR900090

Knote C., Bonafe G. & Di Giuseppe F. (2009) - *Leaf area index specification for use in mesoscale weather prediction systems.* Monthly Weather Review, **137**(10): 3535-3550. https://doi.org/10.1175/2009MWR2891.1

Lu N. & Godt J. (2008) - *Infinite slope stability under steady unsaturated seepage conditions.* Water Resour Res., **44**: 11.

Masi E. B., Segoni S. & Tofani V. (2021) - *Root reinforcement in slope stability models: a review*. Geosciences, **11**(5): 212. https://doi.org/10.3390/geosciences11050212

Masi E. B., Tofani V., Rossi G., Cuomo S., Wu W., Salciarini D., ... & Catani F. (2023) - *Effects of roots cohesion on regional distributed slope stability modelling*. Catena, **222**: 106853. https://doi.org/10.1016/j.catena.2022.106853

Pack R., Tarboton D. & Goodwin C. (2001) - *Assessing terrain stability in a GIS using SINMAP*. In: 15th Annual GIS Conference, GIS, 2001

Park H.J., Lee J.H. & Woo I. (2013) - *Assessment of rainfall-induced shallow landslide susceptibility using a GIS-based probabilistic approach*. Engineering Geology, **161**: 1-15. https://doi.org/10.1016/j.enggeo.2013.04.011

Rossi G., Catani F., Leoni L., Segoni S. & Tofani V. (2013) - *HIRESSS: a physically based slope stability simulator for HPC applications.* Natural Hazards and Earth System Sciences, **13**(1): 151-166. https://doi.org/10.5194/nhess-13-151-2013

Salciarini D., Fanelli G. & Tamagnini C. (2017) - *A probabilistic model for rainfall-induced shallow landslide prediction at the regional scale.* Landslides, **14**: 1731-1746. https://doi.org/10.1007/s10346-017-0812-0

Salvatici T., Tofani V., Rossi G., D'ambrosio M., Tacconi Stefanelli C., Masi E. B., ... & Casagli N. (2018) - *Application of a physically based model to forecast shallow landslides at a regional scale*. Natural Hazards and Earth System Sciences, **18**(7): 1919-1935. https://doi.org/10.5194/nhess-18-1919-2018

Simoni S., Zanotti F., Bertoldi G. & Rigon R. (2008) - *Modelling the probability of occurrence of shallow landslides and channelized debris flows using geotop-fs*. Hydrol. Process., **22**: 532-545. https://doi.org/10.1002/hyp.6886

StatsClimat (2025) - *Climatological report for Aosta, Italy*. Available at https://statsclimat.com/Europe/Italy/report_Aosta

Tofani V., Masi E. B. & Rossi G. (2023) - *Physically-based regional landslide forecasting modelling: model set-up and validation.* Progress in Landslide Research and Technology, **2**: 127-135.

Wu J., Liu L., Sun C., Su Y., Wang C., Yang J., ... & Zhang H. (2019). Estimating rainfall interception of vegetation canopy from MODIS imageries in Southern China. Remote Sensing, **11**(21): 2468. https://doi.org/10.3390/rs11212468

Received January 2026 - Accepted May 2026